Multiple Scattering of Fast Charged Particles*

H. S. SNYDER AND W. T. SCOTT**
Brookhaven National Laboratory, Upton, New York
(Received February 11, 1949)

The theory of multiple scattering of charged particles has been extended in the small-angle approximation valid for thin foils and fast particles. The extension consists of an exact solution of the integral diffusion equation for the correlated probabilities of lateral and angular displacements, and the numerical integration of the resulting expression for the angular distribution. The projection of the scattering on a plane has been used for simplicity. The results are expressed in terms of dimensionless variables η/η_0 and z/λ representing respectively the deflection angle in terms of a small unit determined by the screening, and the foil thickness in terms of the mean free path for scattering. Numerical calculations for values of z/λ from 100 to 84,000, and for an adequate range of η/η_0, have been carried out, and tables have been made available. Curves are presented for a few values of z/λ. The matching is shown between the approximately Gaussian result for small angles and the Rutherford single scattering result valid for large angles. The deviations of the new results from each of these limiting values is quite large over a wide range of angle. An explicit asymptotic formula for large η is given, showing correction terms to the single scattering formula.

1. INTRODUCTION

THE theory of the multiple scattering of charged particles has been treated by several authors.[1] In the present paper the work of these authors has been extended in certain directions at the expense of simplifying assumptions. The major simplifying assumption is that the scattering angle is small; this assumption limits the validity of the results obtained to high energy particles and thin scattering foils, and entails the complete disregard of back scattering and re-entrant particles. The second simplifying assumption is that the scattering cross section is given by the Born approximation for a potential field of the form $V=(ze^2/r)\exp(-r/a)$, the exponential factor representing the screening effect. Energy loss by the particles is neglected. The calculations also have been simplified by taking the projection of the scattering distribution on a fixed plane.

The main objective of this investigation was to determine precisely the manner in which the large angle Rutherford scattering fits on to the small angle highly multiple scattering. We have as a by-product of this investigation obtained accurate angular distributions for the scattered particles for a large number of foil thicknesses. In addition, for large scattering angles an approximate expression was found for the scattering distribution which gives good results when the actual distribution differs from the Rutherford distribution by less than 20 percent.

2. THE DIFFUSION EQUATION

Since Rutherford scattering is predominantly forward, we assume that the incident direction of the particle is the z-direction, that the foil is perpendicular to the z-axis, and that the total angular deviation of the scattered particle is sufficiently small so that we may approximate $\cos\theta$ by 1 and $\sin\theta$ by θ. Let $W(\eta, \epsilon, x, y|z)d\eta d\epsilon dxdy$ represent the probability that a particle initially traveling along the z-axis at $z=0$, pass through the area $dxdy$ at the point (x, y, z), traveling in a direction determined by η to $\eta+d\eta$ and ϵ to $\epsilon+d\epsilon$. η and ϵ are respectively the angles made with the z-axis by the projections of the track in the xz and yz planes. This function satisfies a well-known diffusion equation, written here with the small angle approximation:[2]

$$\left(\frac{\partial}{\partial z}+\eta\frac{\partial}{\partial x}+\epsilon\frac{\partial}{\partial y}\right)W(\eta, \epsilon, x, y|z)$$
$$=N\int_{-\infty}^{\infty}d\eta'\int_{-\infty}^{\infty}d\epsilon'\sigma(((\eta-\eta')^2+(\epsilon-\epsilon')^2)^{\frac{1}{2}})$$
$$\times[W(\eta', \epsilon', x, y|z)-W(\eta, \epsilon, x, y|z)] \quad (1)$$

where $\theta=((\eta-\eta')^2+(\epsilon-\epsilon')^2)^{\frac{1}{2}}$ signifies an angle of single scattering, $\sigma(\theta)$ is the single scattering cross section per unit solid angle and N is the density of scattering centers.

Forming

$$W(\eta, x|z)=\int_{-\infty}^{\infty}\int_{-\infty}^{\infty}d\epsilon d\eta W(\eta, \epsilon, x, y|z) \quad (2)$$

we find that

$$\left(\frac{\partial}{\partial z}+\eta\frac{\partial}{\partial x}\right)W(\eta, x|z)=N\int_{-\infty}^{\infty}\sigma_{\text{proj.}}(\eta-\eta')$$
$$\times\{W(\eta', x|z)-W(\eta, x|z)\}d\eta' \quad (3)$$

where

$$\sigma_{\text{proj.}}(\eta)=\int_{-\infty}^{\infty}\sigma((\eta^2+\epsilon^2)^{\frac{1}{2}})d\epsilon. \quad (4)$$

The function $W(\eta, x|z)$ is the distribution function for the projection of the scattering on the xz plane. Equa-

* Work done at the Brookhaven National Laboratory under contract with AEC.
** Now at Smith College, Northampton, Massachusetts.
[1] E. J. Williams, Proc. Roy. Soc. **169**, 531 (1939); S. Goudsmit and J. L. Saunderson, Phys. Rev. **57**, 24 (1940); **58**, 36 (1940).

[2] W. T. Scott, Phys. Rev. **75**, 212 (1949) and references 2, 3, and 4 of that paper. Note the different notation in this paper.

tion (3) can also be written

$$\left(\frac{\partial}{\partial z}+\frac{\partial}{\partial x}\right)W(\eta, x|z)$$

$$=\frac{1}{\lambda}\int_{-\infty}^{\infty}\{W(\eta', x|z)-W(\eta, x|z)\}p(\eta-\eta')d\eta' \quad (5)$$

where $p(\eta)d\eta$ is the probability that a particle will be scattered in a single scattering into a range between η and $\eta+d\eta$, and λ is the mean free path for scattering with[3]

$$\frac{1}{\lambda}=N\int_{-\infty}^{\infty}\sigma_{\text{proj.}}(\eta)d\eta, \quad \text{and} \quad p(\eta)=N\lambda\sigma_{\text{proj.}}(\eta). \quad (6)$$

The solution of Eq. (5) corresponding to the boundary condition that

$$W(\eta, x|z)=\delta(x)\delta(\eta), \text{ when } z=0$$

is

$$W(\eta, x|z)=\frac{1}{4\pi^2}\int_{-\infty}^{\infty}ds\int_{-\infty}^{\infty}dt \times\exp\left\{i(\eta s+xt)-\frac{h(s+tz)-h(s)}{\lambda t}\right\} \quad (7)$$

in which

$$h(s)=\int_0^s[1-q(s)]ds \quad (8)$$

and

$$q(s)=\int_{-\infty}^{\infty}e^{i\eta s}p(\eta)d\eta.$$

This solution was obtained by applying a Laplace transform in z and Fourier transforms in x and η to Eq. (5), solving the resulting first-order ordinary differential equation, and then evaluating the inverse Laplace transform. Equation (7) is easily checked by substitution into (5).

Integrating (8) with respect to x we obtain the angular distribution

$$W(\eta|z)=\int_{-\infty}^{\infty}W(\eta, x|z)dx$$

$$=\frac{1}{2\pi}\int_{-\infty}^{\infty}\exp\left[i\eta s+\frac{z}{\lambda}(q(s)-1)\right]ds$$

$$=\frac{1}{\pi}\int_0^{\infty}\cos\eta s\exp\left[\frac{z}{\lambda}(q(s)-1)\right]ds$$

$$=\text{Real Part}\left\{\frac{1}{\pi}\int_0^{\infty}\exp\left[i\eta s+\frac{z}{\lambda}(q(s)-1)\right]ds\right\}. \quad (9)$$

[3] This use of the symbol λ must not be confused with that in the paper of reference 2.

3. THE CROSS SECTION AND $q(s)$

If we use the potential of the form $V=(ze^2/r)\times\exp(-r/a)$ we find that the differential scattering cross section per unit solid angle becomes

$$\sigma(\theta)=\frac{z^2z'^2e^4}{\mu^2c^4(E-1/E)^2[\sin^2\theta/2+(\eta_0/2)^2]^2}$$

$$\cong\frac{4z^2z'^2e^4}{\mu^2c^4(E-1/E)^2[\theta^2+\eta_0^2]^2} \quad (10)$$

in which

$$\eta_0=\frac{\hbar}{a\mu c(E^2-1)^{\frac{1}{2}}}. \quad (11)$$

In the above equations E is the total energy of the charged particle, measured in units of its rest mass, μ is its rest mass, and $z'e$ is its charge. The constant a, the screening radius, may be given its conventional value

$$a=a_0/z^{\frac{1}{3}}=\hbar^2/mez^{\frac{1}{3}} \quad (12)$$

in which a_0 is the Bohr radius of hydrogen.

Using the value of $\sigma(\theta)$ given by (10) we find for λ the value

$$\frac{1}{\lambda}=\frac{4z^2z'^2e^4N\pi}{\mu^2c^4(E-1/E)^2\eta_0^2} \quad (13)$$

and for the projected scattering probability

$$p(\eta)=\frac{\eta_0^2}{2(\eta^2+\eta_0^2)^{\frac{3}{2}}}. \quad (14)$$

Thus

$$q(s)=\tfrac{1}{2}\int_{-\infty}^{\infty}\frac{e^{i\eta s}\eta_0^2d\eta}{(\eta^2+\eta_0^2)^{\frac{3}{2}}}$$

$$=\tfrac{1}{2}\int_{-\infty}^{\infty}\frac{e^{i\eta_0sx}dx}{(1+x^2)^{\frac{3}{2}}}=-s\eta_0K_1(\eta_0s). \quad (15)$$

In Eq. (15) K_1 is the modified Bessel function of the first kind.[4] The power series expansion for $q(s)-1$ is

$$q(s)-1=\frac{(s\eta_0)^2}{2}\left\{\ln\left(\frac{s\eta_0}{2}\right)+0.0772157\cdots\right\}$$

$$+\frac{(s\eta_0)^4}{16}\left\{\ln\left(\frac{s\eta_0}{2}\right)-0.6727843\cdots\right\}$$

$$+\frac{(s\eta_0)^6}{384}\left\{\ln\left(\frac{s\eta_0}{2}\right)-1.089451\cdots\right\}+\cdots. \quad (16)$$

By observing the form of (15) and of (9) one sees that $W(\eta|z)$ is a function of η/η_0 and z/λ so that measuring

[4] Watson, *Bessel Functions* (1945), pp. 80, 172.

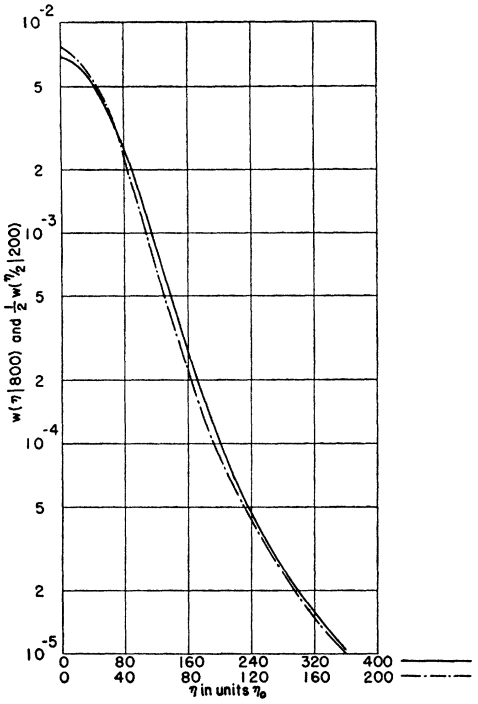

FIG. 1. Plot of $W(\eta|800)$ and $\frac{1}{2}W(\eta/2|200)$ to show the effect of changing the screening radius by a factor two. η represents the angle in units of η_0.

z in units of λ, and η in units of η_0, then the functions $W(\eta|z)$ have a universal form in which z becomes the average number of collisions which the particle undergoes in passing through the foil. This result amounts to setting $\lambda=\eta_0=1$ in the various formulas, which will be done in the rest of this paper. It should be noted that a change in η_0 requires a renormalization of $W(\eta|z)$.

4. AN APPROXIMATION FOR $W(\eta|z)$

It has been pointed out many times that for sufficiently large angles the distribution function in the case of Rutherford scattering should approach the single scattering law multiplied by the average number of times the particle has been scattered. That is,

$$W(\eta|z)\cong z/2\eta^3, \text{ for large } \eta. \tag{17}$$

We now verify this result, and in addition obtain correction terms to (17). Deforming the path of integration in Eq. (9) to the imaginary axis we may write

$$W(\eta|z)=\text{Real Part}\left\{\frac{i}{\pi}\int_0^\infty \exp(-\eta t+z(q(it)-1))dt\right\}$$

$$=\text{Real Part}\left\{\frac{i}{\pi}\int_0^\infty dt\{e^{-\eta t}[1+z\{q(it)-1\}$$

$$+z^2/2\{q(i\theta)-1\}^2+z^3/6\{q(it)-1\}^3+\cdots]\}\right\}. \tag{18}$$

Using the value of $q(s)-1$ given by the first term of (16) we then get

$$W(\eta|z)\cong\text{Real Part}\left\{\frac{i}{\pi}\int_0^\infty dte^{-\eta t}\right.$$

$$\times\left[1-\frac{zt^2}{2}\left(\ln t/2+\frac{\pi i}{2}+0.077215\right)\right.$$

$$+\frac{z^2t^4}{8}\left(\ln t/2+\frac{\pi i}{2}+0.077215\right)^2$$

$$\left.\left.-\frac{z^3t^6}{48}\left(\ln t/2+\frac{\pi i}{2}+0.077215\right)^3+\cdots\right]\right\}. \tag{19}$$

Thus

$$W(\eta|z)=z/4\int_0^\infty t^2e^{-\eta t}dt$$

$$-z^2/8\int_0^\infty t^4e^{-\eta t}\{\ln t/2+0.077215\}$$

$$+z^3/32\int_0^\infty t^6e^{-\eta t}\left\{(\ln t/2+0.077215)^2-\frac{\pi^2}{12}\right\}+\cdots, \tag{20}$$

or

$$W(\eta|z)=z/2\eta^3[1+6z/\eta^2(\ln\eta-0.8840)$$

$$+45z^2/\eta^4\{(\ln\eta+0.616)^2$$

$$-3.852(\ln\eta+0.616)+3.334\}+\cdots]. \tag{21}$$

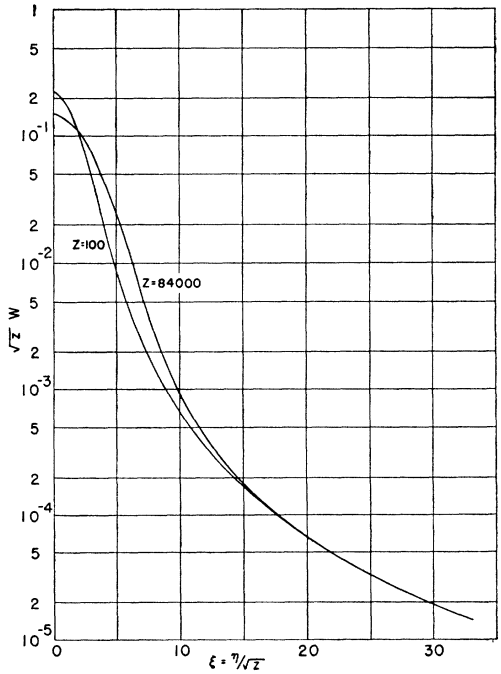

FIG. 2. Semi-logarithmic graphs of $W(\eta|z)$ for $z=100$ and 84000. (z in units of the mean free path for scattering.) $(z)^{\frac{1}{2}}W$ is plotted as a function of $\xi=\eta/(z)^{\frac{1}{2}}$.

TABLE I. $W(\eta|z)$ as a function of η for $z=100$.

η	$W(\eta\|100)\times10^6$	η	$W(\eta\|100)\times10^6$
0	22850	145	18.53
5	21730	150	16.62
10	18740	155	14.96
15	14770	160	13.52
20	10780	165	12.26
25	7422	170	11.15
30	4904	175	10.18
35	3170	180	9.312
40	2041	185	8.542
45	1331	190	7.856
50	888.4	195	7.242
55	608.6	200	6.691
60	430.0	205	6.195
65	314.5	210	5.747
70	236.3	215	5.341
75	180.5	220	4.973
80	140.8	225	4.638
85	113.4	230	4.333
90	93.34	235	4.054
95	76.91	240	3.798
100	63.92	250	3.349
105	53.78	260	2.968
110	45.96	270	2.643
115	39.60	280	2.364
120	34.38	290	2.123
125	30.04	300	1.913
130	26.42	310	1.731
135	23.36	320	1.571
140	20.76	330	1.430

In Eq. (21) we have neglected terms of order $1/z$ as compared to unity as we used only the first term in series (16). Comparison of the results given by (21) with values obtained by the numerical integration of Eq. (9) shows that (21) gives accurate results provided

$$6z/\eta^2(\ln\eta-0.8840)<0.2. \tag{22}$$

However, when the expression (22) is larger than 0.3 the errors in (21) are quite large.

5. NUMERICAL CALCULATIONS

The values of $W(\eta|z)$ were calculated for small values of η by numerical integration of Eq. (9). The power series for $q(s)-1$ given by Eq. (16) was used for its calculation. For large values of η the approximate formula (21) was used. The numerical integration of (9) to give $W(\eta|z)$ was done for $z=100$, 1500, 3000 and 9000. The major difficulty with the use of (9) for numerical work is that the factor $\cos(\eta s)$ oscillates very rapidly for large values of η with the consequence that very high accuracy is required for the integrand in order that reasonable accuracy is obtained in the final results. In fact $q(s)-1$ had to be computed up to ten significant figures in order that the value of $W(\eta, s)$ would be accurate to three significant figures at the place where the approximate formula (21) overlapped the results of the

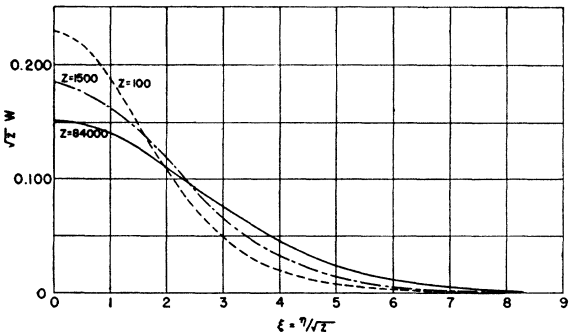

FIG. 3. Linear graphs of $z(W)^{\frac{1}{2}}$ against ξ for $z=100$, 1500, and 84,000.

numerical integrations. The values of $W(\eta|z)$ for other values of z were computed by means of the formula

$$W(\eta|z_1+z_2)=\int_{-\infty}^{\infty} W(\eta|z_1)W(\eta-\eta'|z_2)d\eta'. \tag{23}$$

Once one has obtained a table of values of $W(\eta|z)$ for a particular $z=z_1$, then $W(\eta|z)$ may be computed for $z=2z_1$, $3z_1$, $4z_1\cdots$ with about one-thirtieth of the labor that is required in the use of Eq. (9). The distribution functions as given in the tables should be accurate to better than 1 percent. The major uncertainty in the values arises from the fact that with repeated application of (23) the errors accumulate. The above estimate of the accuracy is supported by the fact that the areas under the curves, $\int_{-\infty}^{\infty} W(\eta|z)d\eta$, as computed numerically, were in all cases in error by less than 1 percent.

TABLE II. $W(\eta|z)$ as a function of η for $z=1500$.

η	$W(\eta\|1500)\times10^6$
0	4786
50	3931
100	2192
150	912.1
200	327.1
250	121.6
300	53.13
350	27.81
400	16.47
450	10.70
500	7.405
550	5.360
600	3.993
650	3.080
700	2.450
750	1.970
800	1.596
850	1.313
900	1.100
950	0.9300
1000	0.7950

6. EFFECTS OF CHANGE IN SCREENING RADIUS

The precise value which should be used for the screening radius, a, is not known, although it may be estimated by using Eq. (12). The value of the screening radius as given by (12) should be accurate to within ten percent. In addition, the precise manner in which Rutherford cross section should be cut off at small angles is not known. In Fig. 1 we show some results of changing the screening radius by a factor of two, thus changing η_0 by two and λ by four. The dashed curve is $\frac{1}{2}W[(\eta/2)|200]$ and the solid curve is $W(\eta|800)$. The dashed curve thus shows the angular distribution for the same physical angles, the same particle energy and foil thickness but with one quarter the total cross section of the solid curve. For $\eta=0$ the difference between these functions is only seven percent. The maximum difference is about thirty percent. At greater foil thickness the difference between these functions would have been even smaller. Since the total cross section as determined by (12) may be reasonably assumed to be in error by less than 20 percent we felt quite confident that the functions $W(\eta|z)$ as computed by this method are, for $z>100$, in error by less than two percent as a result of uncertainties in the screening effect.

TABLE III. $W(\eta|z)$ as a function of η for $z=84{,}000$.

η	$W(\eta\|84{,}000)\times10^6$
0	523.0
200	504.4
400	451.7
600	374.7
800	289.9
1000	210.5
1200	144.1
1400	93.23
1600	58.03
1800	35.33
2000	21.36
2200	13.05
2400	8.228
2600	5.433
2800	3.765
3000	2.725
3200	2.053
3400	1.599
3600	1.278
3800	1.039
4000	0.8611
4200	0.7221
4400	0.6132
4600	0.5245
4800	0.4544
5000	0.3965
5200	0.3482
5400	0.3075
5600	0.2730

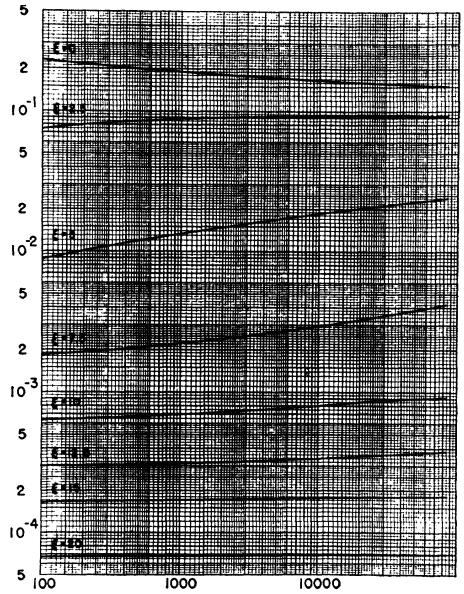

FIG. 4. Logarithmic graphs of $z(W)^{\frac{1}{2}}$ against z for eight values of $\xi=\eta/(z)^{\frac{1}{2}}$.

7. TABLES AND GRAPHS

The tables and graphs make use of the following measures of angle and thickness:

1. The angle η which is the angle of scattering projected on a plane containing the incident direction is measured in units η_0. From Eqs. (11) and (12) we have $\eta_0=(m/\mu)z^{\frac{1}{2}}/137(E^2-1)^{\frac{1}{2}}$ radians. In this formula m is the mass of the electron, μ the mass of the incident particle, z the charge of the scattering nucleus and E the energy of this incident particle, including its rest energy, in units μc^2.

2. The thickness z of the scattering foil is measured in units of the mean free path λ given by Eq. (13):

$$1/\lambda=9.86\times10^{-25}N(m/\mu)^2z^2z'^2/(E-1/E)^2\eta_0^2 \text{ cm}^{-1}.$$

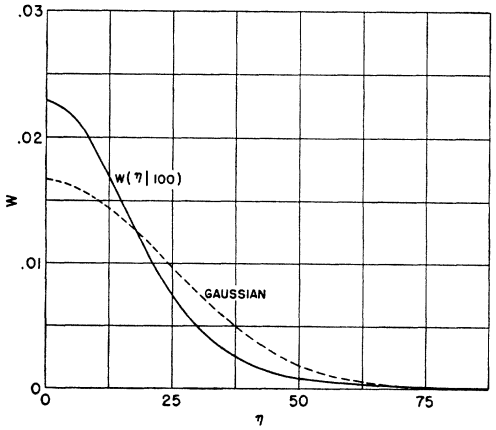

FIG. 5. Linear graphs of $W(\eta|100)$ and the Gaussian curve $W=(1/1151\pi)^{\frac{1}{2}}\exp(-\eta^2/1151)$ as functions of η.

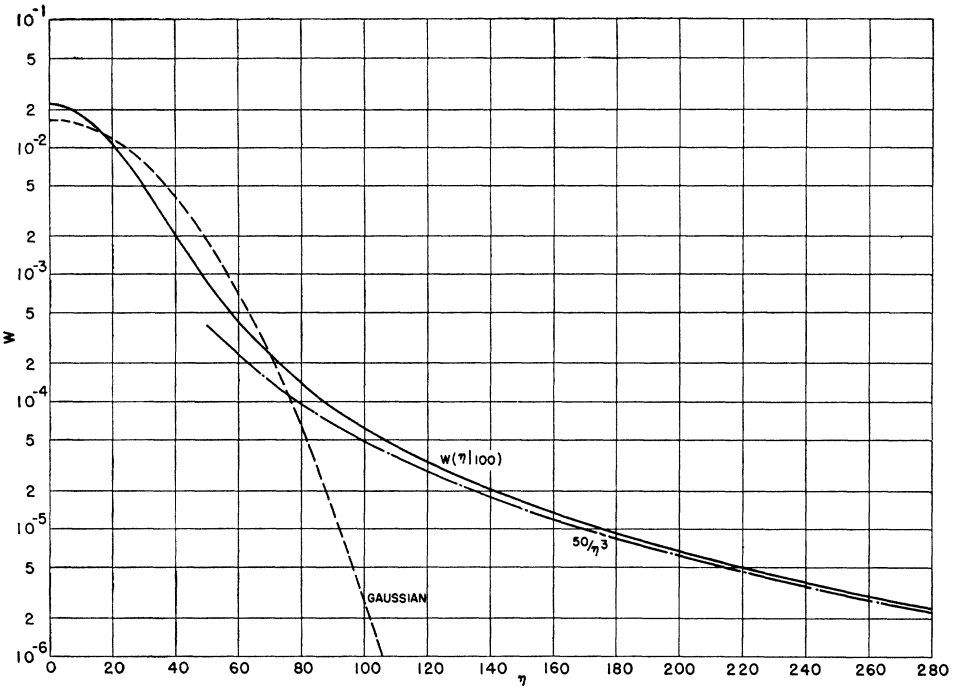

FIG. 6. Semi-logarithmic graphs of $W(\eta|100)$, the Gaussian curve of Fig. 5, and the single scattering approximation $W\simeq 50/\eta^3$, as functions of η.

Here N is the number of atoms per cc in the scattering foil and $z'e$ the charge of the incident particle.

We give in Tables I to III values of $W(\eta|z)$ for three sample values of z: 100, 1500, 84000. Figure 2 gives logarithmic graphs for $z=100$ and $z=84000$; $(z)^{\frac{1}{2}}W$ is here plotted as a function of $\xi=\eta/(z)^{\frac{1}{2}}$ to show the similarity between the two curves with this method of plotting.[5] This similarity is of course already revealed in Fig. 1. Figure 3 shows the upper part of the curves for the three values of z above, on a linear scale, with the same variables plotted. Neither method of plotting is useful for interpolation. We give in Fig. 4 graphs of $(z)^{\frac{1}{2}}W$ against z for eight values of $\xi=\eta/(z)^{\frac{1}{2}}$, which are more practicable for interpolation. These curves also serve to indicate the accuracy of the calculations, since they are smooth to within 2 percent or better. Complete tables for twenty-nine values of z from 100 to 84000 are available elsewhere.[6]

The relation of the new results to the Gaussian approximation is shown in Figs. 5 and 6, for $z=100$. For the Gaussian curve, we have used reference 2, Eqs. (5) and (13). The logarithm involved is evaluated for a 2 Mev electron in aluminum. It is clear that although the Gaussian curve is a reasonable approximation for small angles, the deviation at large angles is of a large order. In our example, $\eta_0\cong 0.0035$ radians $\cong 0.2$ degree. For $\eta=100$ or an angle of $\cong 20°$, the Gaussian result is 0.044 of our value.

The deviations from the single scattering result are also shown in Fig. 6, which includes a graph of $W=50|\eta^3$ (Eq. (17) for $z=100$). It is especially noteworthy to observe how slowly our distributions approach this result; even for small thicknesses z, one has to go to large angles η. For example, for $z=100$ the first correction term in Eq. (21) still amounts to 5 percent for $\eta=230$, where the scattered intensity is only 0.02 percent of the central maximum. For $z=600$ this occurs at $\eta=640$ where the intensity is reduced to 0.015 percent. Choosing as an actual example the scattering of electrons of about 2 Mev kinetic energy by an aluminum foil of about 0.0001 inch thickness, we find $\eta_0\cong 0.0035$ radians, $1/\lambda\cong 3.6\times 10^5$ cm^{-1}, $z\cong 90$. In this case the deviation from single scattering is down to 5 percent for $\eta=210$, corresponding to a scattering angle of over 40 degrees. This is beyond the small angle approximation used in the present treatment but shows nevertheless that single scattering is reached only for very large angles.

The authors wish to express their thanks to Theresa Danielson, Ardith Kenney, and Jean Snover for the numerical calculations.

[5] This method of plotting yields identical curves for different z in the Gaussian approximation.

[6] The tables may be obtained for a charge of ten cents from the Information and Publications Division, Brookhaven National Laboratory, Upton, Long Island, New York.